

## Measurements of charge transfer and target-electron-loss cross sections for $H^+$ , $D^+$ , and $He^+$ impact on lithium at low energies

Paul Oxley <sup>\*</sup>*Department of Physics, The College of the Holy Cross, Worcester, Massachusetts 01610, USA*

(Received 22 December 2021; accepted 11 March 2022; published 31 March 2022)

Experimental cross section measurements for charge transfer and for electron loss from lithium via charge transfer and direct ionization are reported for collisions between light ions and lithium atoms. Beams of protons, deuterium ions, and helium ions intersect a lithium atom beam, and collision cross sections are inferred by measuring the number of lithium ions produced in the collisions. The collision energy ranges studied are 0.13–3.5 keV for proton impact, 0.13–0.83 keV for deuterium ion impact, and 0.28–3 keV for helium ion impact. At proton collision energies below 0.7 keV our charge transfer cross sections are in excellent agreement with the theoretical predictions, resolving a long-standing discrepancy between theory and experiment in this energy range. Cross sections for proton and for deuterium ion impact on lithium are measured to be identical when scaled to the same collision velocity, indicating that quantum effects are not significant in the energy range studied. Comparison between our cross section measurements for lithium electron loss due to helium ion impact and previously measured charge transfer cross sections show that ionization is a negligible process in  $He^+ + Li$  collisions at energies below 3 keV. Undulations in the measured collision cross sections at low energy are observed for both proton and helium ion impact and are compared to molecular orbital close-coupling calculations.

DOI: [10.1103/PhysRevA.105.032824](https://doi.org/10.1103/PhysRevA.105.032824)

### I. INTRODUCTION

Ion-atom charge transfer collisions occur in a wide range of physical environments, from the interstellar medium [1] and the tails of comets [2], to tokamak [3] and antimatter [4] plasmas. A thorough understanding of charge transfer collisions requires theoretical and experimental studies of collision systems that are amenable to accurate calculation and can be conveniently created in the laboratory. Singly charged ions impacting on quasi-one-electron alkali-metal atom targets satisfy these requirements. Charge transfer between hydrogen ions and lithium atoms in particular has applications in tokamak plasma devices. Charge exchange spectroscopy with neutral lithium beams is used as a plasma diagnostic in such devices [5–8], while liquid lithium coating of plasma facing components is an active area of tokamak research [9–15]. In both applications understanding collisional interactions between lithium atoms and plasma ions is of great importance.

The work presented here details measurements of charge transfer cross sections for lithium-proton collisions at energies between 0.13 and 3.5 keV (lab frame), with a focus on measurements at the lower end of this energy range. We also present measurements of charge transfer cross sections for lithium-deuterium ion collisions (0.13–0.83 keV energy range) and lithium-electron-loss cross sections for lithium-helium ion collisions (0.28–3 keV energy range).

Multiple experimental studies exist for lithium-proton charge transfer at collision energies greater than 2 keV [16–19], and agreement between these measurements and theoretical predictions [20–25] is good. However, only one of

these experiments studied collisions below 2 keV [16] and the experimental results deviate from most of the theoretical predictions as the collision energy is reduced below about 0.7 keV. To our knowledge, only one experiment has studied charge transfer between lithium atoms and deuterium ions [19] while several experimental studies of lithium-helium ion charge transfer exist [16–18] but again only one of these experiments studied collisions below 2 keV [16].

### II. EXPERIMENTAL METHOD

The experimental setup used in our collision studies is shown in Fig. 1. We used a crossed-beams technique in which the ion beam under study intersected an atomic lithium beam at right angles. Lithium ions generated in the collision were guided by electric fields to a channel electron multiplier (CEM) and output pulses from the CEM were amplified, discriminated, and counted to infer the collision cross section.

The beam of ions was generated in a radio-frequency discharge source. Ions were extracted from the discharge at the desired collision energy and then filtered by a Wien charge-to-mass filter. To achieve collision energies below 1 keV the ion beam passed through a Menzinger-type decelerator (not shown in Fig. 1) before it intersected the lithium beam. The Wien filter allowed the isolation of pure proton and  $He^+$  beams, but could not separate  $D^+$  and  $H_2^+$  ions (which result from dissociated water vapor in the ion source). However, with an appropriate choice of argon-deuterium gas mixture and rf discharge power for the source, we are confident that  $H_2^+$  contributed less than 2% of the  $D^+$  beam current.

The ion beam current was measured by a beveled Faraday cup built according to the design detailed in [26]. This design is highly effective at preventing secondary electrons escaping

poxley@holycross.edu

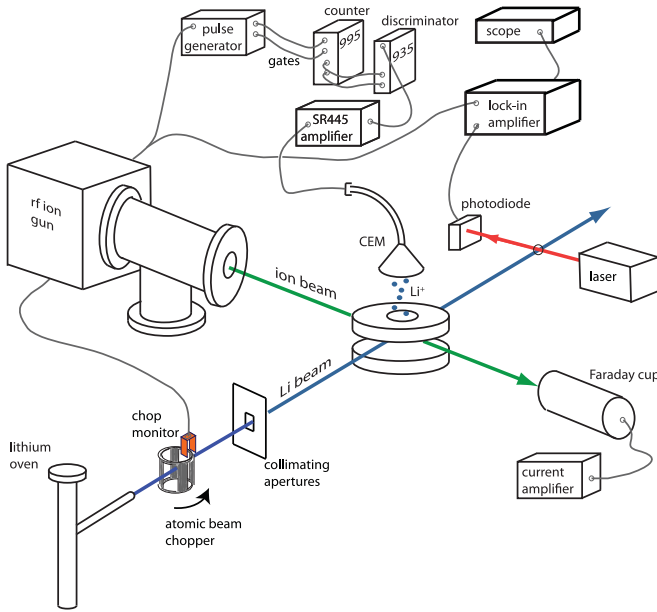


FIG. 1. Schematic of the experimental apparatus.

the cup, and in our apparatus we measured the fraction of secondaries to be less than 1% of the ion current. Measurements of the beam energy using a biased Faraday cup allowed us to account for the plasma potential of the rf discharge, which was found to be  $32 \pm 7$  eV. The size of the ion beam was defined by a 3-mm-diameter aperture placed close to the collision site.

The lithium atomic beam was produced in an oven designed for use in cold atom experiments [27,28]. The oven was heated to 575 °C and produced a partially collimated lithium beam. Further collimation was provided by apertures positioned between the oven and the collision site, resulting in a rectangular-shaped lithium beam of thickness 3 mm (in the direction of travel of the ion beam) and height 10 mm. The overlap volume of the two beams was therefore a cylinder of diameter 3 mm and length 3 mm.

An important feature of our experiment was the rotating chopper that intercepted the lithium beam on its way to the collision site. Chopping the lithium beam allowed for back-

ground subtraction of ions produced in collisions between the ion beam and background gas atoms in the collision vacuum chamber. In addition, chopping the lithium beam allowed precise measurements of the lithium beam density, integrated along the direction of the ion beam travel. This was done by passing a laser through the lithium beam and measuring the transmitted laser power as its frequency was swept across the  $2S_{1/2} \rightarrow 2P_{3/2}$  lithium transition, as is described in detail in [29]. At the collision site the atomic beam density was typically  $3 \times 10^8$  atoms/cm<sup>3</sup>.

A vertical electric field of 6 V/cm was applied at the collision site. This field, along with additional fields in the region above the collision site, was used to steer lithium ions produced in collisions onto the CEM. Simulations using the SIMION field and particle trajectory simulator showed that over 99.9% of lithium ions created at the collision site will reach the CEM, and given a chamber pressure of  $4 \times 10^{-8}$  Torr, the probability of a lithium ion being neutralized on its path to the CEM is negligible. A Li<sup>+</sup> detection efficiency of 90% was due to the efficiency of the CEM itself, and this value is taken from efficiency measurements of a CEM almost identical to ours [30]. The 6-V/cm field determined the lowest collision energy used in our studies. With this field and our lowest energy proton beam (130 eV), the protons are deviated by 15% of the lithium beam height. We considered this deviation to be the maximum amount acceptable.

The CEM was operated in pulse-counting mode and the output pulses were amplified, discriminated, and sent to both channels of a two-channel gated counter. One channel was gated when the lithium beam was on (chopper wheel open) and the other when it was off (chopper wheel closed). The difference in counts between the two channels ( $N_{\text{on}} - N_{\text{off}}$ ) allowed us to measure the count rate,  $R_{\text{net}}$ , due to collisions with the lithium atoms only, according to Eq. (1),

$$R_{\text{net}} = \frac{N_{\text{on}} - N_{\text{off}}}{Tf}, \quad (1)$$

where  $T$  is the duration of the experiment and  $f$  is the fraction of time the lithium on gate is present. Correct temporal alignment of the gates and the lithium beam state was confirmed by

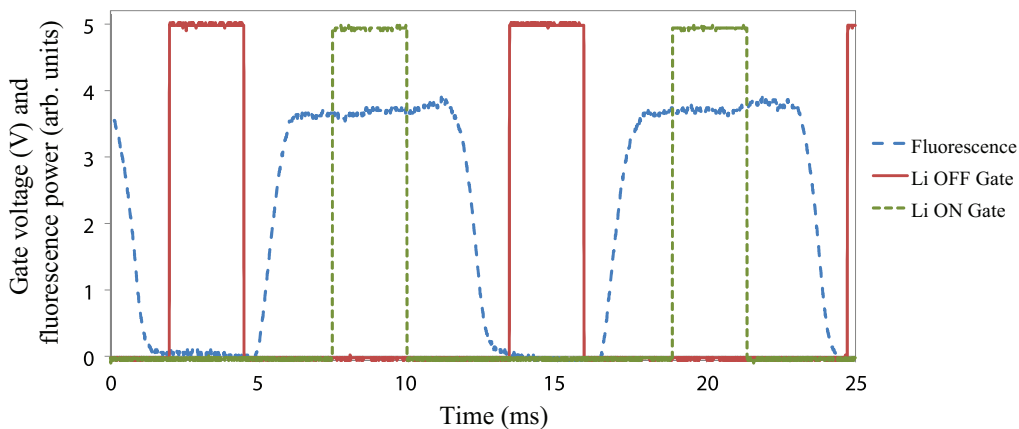


FIG. 2. Gates for counting CEM pulses when the lithium beam is off and on are appropriately timed relative to the lithium atom fluorescence.

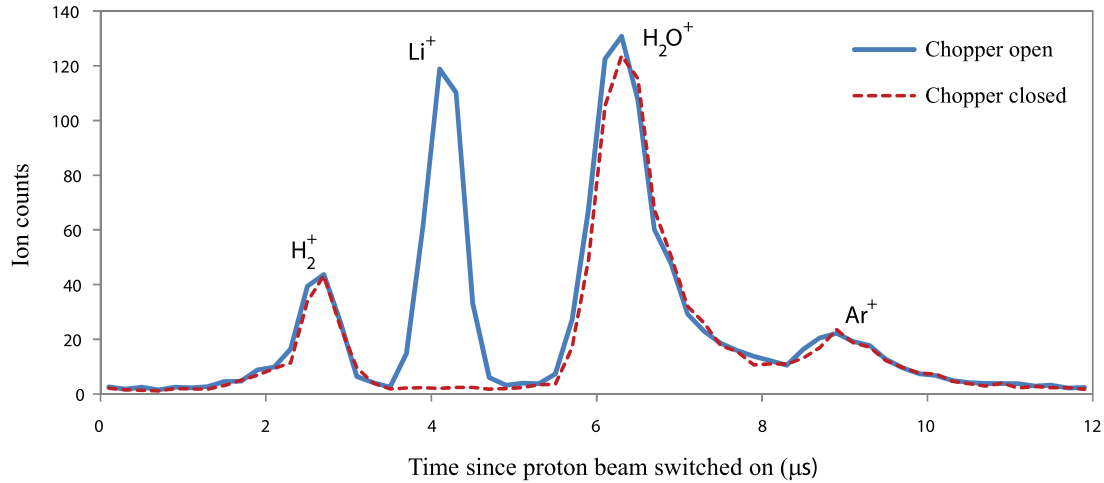


FIG. 3. Searching for contaminant ions present in the lithium beam. Contaminant ions would appear as new peaks in the time of flight spectrum when the chopper is opened.

monitoring laser-induced fluorescence from the lithium beam, as shown in Fig. 2.

We probed for contaminants present in the lithium beam using a time-of-flight technique and a pulsed proton beam. The proton beam was pulsed on and the number of ions detected by the CEM at different times was recorded, both with the chopper open and then closed. The results are shown in Fig. 3. Several ions produced in collisions between protons and background gas can be identified. Argon and hydrogen ions are present due to the mixture of these gases entering the collision vacuum chamber from the ion source (the source was operated with a hydrogen-argon gas mixture), while water ions come from water vapor outgassed from the vacuum chamber walls. The key observation from Fig. 3 is that the only new peak which appears when the chopper is opened is that of  $\text{Li}^+$ . If contaminant atoms or molecules were present in the lithium beam these would be observed as additional peaks.

Since lithium ions are the detected collision product in our experiments, our measured signal comes from two distinct processes:

- (i)  $X^+ + \text{Li} \rightarrow X + \text{Li}^+$  (charge transfer),
- (ii)  $X^+ + \text{Li} \rightarrow X^+ + \text{Li}^+ + e^-$  (ionization),

where  $X^+$  is the incoming hydrogen or helium ion. For proton-lithium collisions in the energy range studied here the ionization cross section is at most a few percent of the charge transfer cross section [31]. This small ionization contribution was accounted for in our analysis, allowing us to infer the charge transfer cross section. Ionization cross sections for the  $\text{He}^+ - \text{Li}$  system are unknown, and so our measurements with  $\text{He}^+$  provide the target-electron-loss cross section [the sum of processes (i) and (ii)].

The experimental uncertainties of our measurements come from uncertainties in the CEM efficiency, the target lithium density, and the measured ion beam current, in addition to statistical uncertainties. Measurements of CEM ion detection efficiencies are relatively scarce [30,32–37], and rather variable due to differences in CEM design and incoming ion

properties. Based on the data provided in these studies, we estimate a CEM detection efficiency uncertainty of 10%, and this is the largest single uncertainty in our experiments. The uncertainty in the lithium target density has two sources—an

TABLE I. Charge transfer cross sections for collisions between lithium atoms and protons ( $\sigma_{\text{H}^+}$ ), and deuterium ions ( $\sigma_{\text{D}^+}$ ); lithium-electron-loss cross sections for singly charged helium ion collisions with lithium ( $\sigma_{\text{He}^+}$ ). Cross section units are  $10^{-15} \text{cm}^2$  and uncertainties quoted are absolute uncertainties.

Energy (keV)	$\sigma_{\text{H}^+}$	$\sigma_{\text{D}^+}$	$\sigma_{\text{He}^+}$
0.13	$0.36 \pm 0.06$	$0.20 \pm 0.03$	
0.18	$0.49 \pm 0.08$		
0.23	$0.52 \pm 0.08$	$0.29 \pm 0.04$	
0.28	$0.60 \pm 0.09$		$0.81 \pm 0.11$
0.29	$0.62 \pm 0.09$		
0.33	$0.72 \pm 0.10$	$0.42 \pm 0.05$	
0.42	$0.88 \pm 0.13$		
0.43	$0.86 \pm 0.12$	$0.46 \pm 0.07$	
0.53	$1.16 \pm 0.17$		$1.94 \pm 0.26$
0.63		$0.62 \pm 0.08$	
0.65	$1.63 \pm 0.22$		
0.73			$2.41 \pm 0.32$
0.75	$1.87 \pm 0.25$		
0.83		$0.75 \pm 0.1$	
0.88	$2.05 \pm 0.27$		
0.93			$3.50 \pm 0.46$
1.03	$2.07 \pm 0.28$		
1.18	$2.19 \pm 0.29$		
1.23			$3.74 \pm 0.49$
1.33	$2.39 \pm 0.32$		
1.53	$2.79 \pm 0.37$		
1.63			$4.91 \pm 0.65$
1.78	$3.34 \pm 0.44$		
2.03	$3.88 \pm 0.52$		$5.73 \pm 0.76$
2.53	$4.63 \pm 0.61$		$6.00 \pm 0.79$
3.03	$5.06 \pm 0.67$		$6.03 \pm 0.80$
3.53	$5.25 \pm 0.70$		

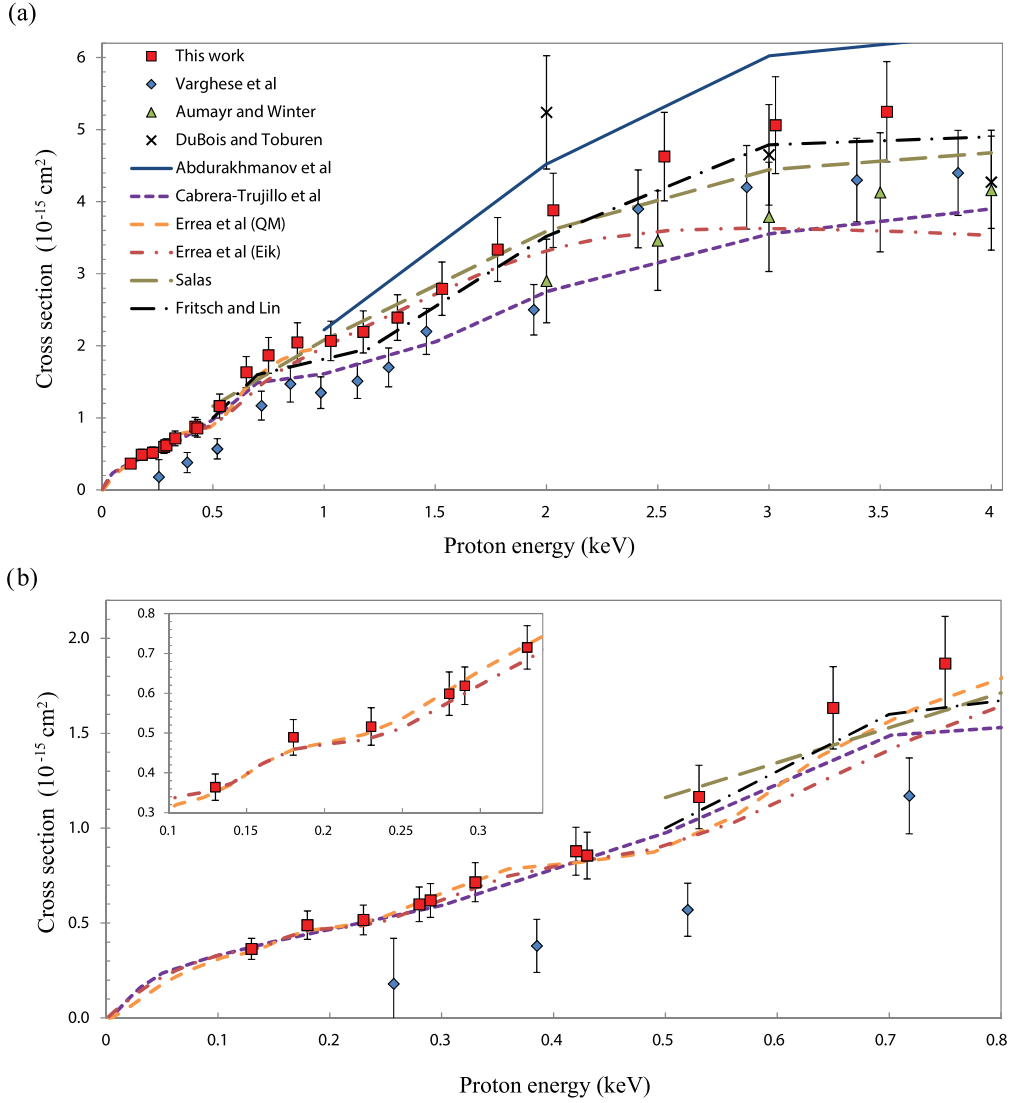


FIG. 4. Proton-lithium charge transfer cross sections. Our work is compared to past measurements: Varghese *et al.* [16], Aumayr and Winter [17], and DuBois and Toburen [18], and to theoretical predictions: Abdurakhmanov *et al.* [22], Cabrera-Trujillo [24], Errea *et al.* [20] quantum (QM) and eikonel (Eik) calculations, Salas [23], and Fritsch and Lin [25].

uncertainty associated with the laser absorption measurement technique, and an uncertainty due to the deviation of the ion beam by the electric field in the collision region which altered the intersection point of the ion and lithium beams. This latter uncertainty is ion beam energy dependent. The uncertainty in the Faraday cup measurement of ion beam current was also energy dependent. The total uncertainty in our measurements range from 13% at beam energies above 500 eV to 15% at energies below 250 eV.

### III. RESULTS AND DISCUSSION

The lithium-electron-loss collision cross section  $\sigma$  was determined from experimentally measured quantities according to Eq. (2),

$$\sigma = \frac{eR_{\text{net}}}{\varepsilon I \int n_{\text{Li}} dz}. \quad (2)$$

In Eq. (2),  $e$  is the elementary charge and  $R_{\text{net}}$  is the background-subtracted lithium ion count rate from Eq. (1). The ion detection efficiency is denoted by  $\varepsilon$ , and is equal to 0.9, and the measured ion beam current is  $I$ . The quantity  $n_{\text{Li}}$  is the density of the lithium beam through which the ion beam passes in the  $z$  direction and the integration is over the thickness of the lithium beam (3 mm). This line-integrated lithium density was measured by laser absorption spectroscopy, as described above.

#### A. Proton-lithium charge transfer cross sections

Lithium-electron-loss cross sections for proton-lithium collisions were determined from Eq. (2) and the charge transfer cross section was found by correcting for the small ionization contribution [31]. Our capture cross section results are shown in Table I, and in Fig. 4 we compare them with prior experimental data and theoretical predictions.

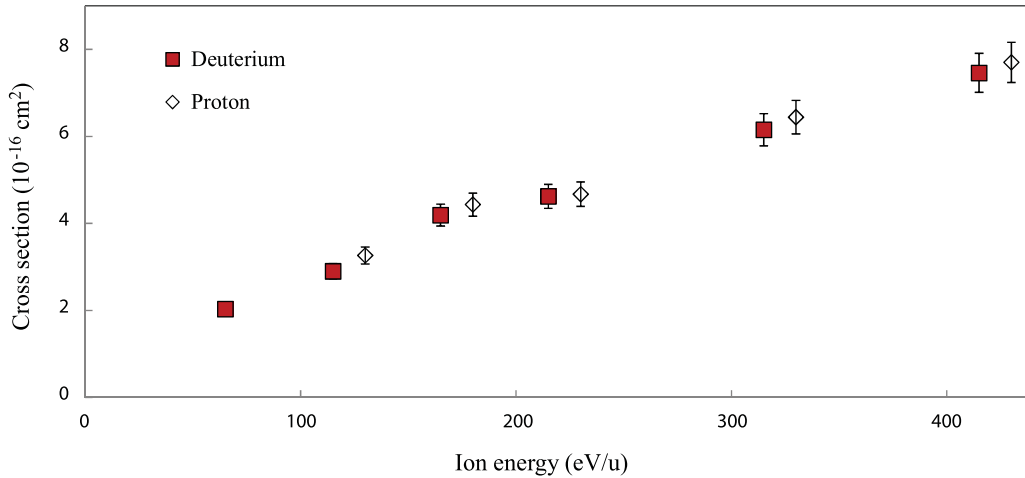


FIG. 5. Comparison of the charge transfer cross section for proton and deuterium ion impact on lithium. Note: at 65 eV/u there is only a measurement for deuterium impact. To better compare proton and deuterium cross sections, the uncertainties shown are relative uncertainties.

Figure 4 can be interpreted by considering three energy ranges. At energies above 2 keV multiple experimental data sets are available and, within the experimental uncertainties, they are in good agreement with each other (except, perhaps, the lowest energy cross section measurement of [18]). In this energy range there is also reasonable agreement between the experimental and theoretical predictions. Between 2 and 0.7 keV, our experimental cross sections agree very well with most theoretical predictions, and are consistently larger than the only previously measured cross sections of Varghese. Below 0.7 keV the theoretical predictions coalesce to a single curve in excellent agreement with our measurements, but significantly above the results of Varghese [Fig. 4(b)].

The discrepancy between our results and those of Varghese could be due to the difference in our experimental methods. The method used by Varghese involved detecting the neutralized protons formed during a charge transfer collision, rather than detecting the lithium ions as was done in our experiments. Both methods have their merits, but at low collision energy the method of Varghese is susceptible to undercounting the neutralized protons if they are scattered beyond the acceptance angle of the detector. This effect is mentioned in [16] and could be the reason for the lower measured cross sections in their work, compared to ours.

A small undulating structure can be seen in our cross section measurements. A “bump” in the cross section at 0.85 keV is clearly present in both our data and those of Varghese [Fig. 4(a)], and has been identified as charge transfer into the  $2p$  orbital of hydrogen during collisions with impact parameters of about 2 a.u. [24]. Our data also show a cross section bump at 0.18 keV [Fig. 4(b), inset]. In order to more meaningfully determine if this is a genuine feature, the uncertainties shown in the inset of Fig. 4(b) include only statistical uncertainties and those which depend on proton energy. Quantum-mechanical molecular-orbital close-coupling calculations of Errea [20] also show a small bump around 0.18 keV, although further analysis of their results would be needed to identify the particular collision process responsible for this feature.

### B. Deuterium-lithium charge transfer cross sections

In addition to our measurements of proton-lithium collision cross sections we studied low energy deuterium-lithium collisions to probe for differences in the charge transfer cross section between hydrogen isotopes. The data are shown in Fig. 5 and were taken during a single experimental session to provide the best possible comparison between measurements of the two isotopes. The deuterium cross sections are given in Table I.

It is expected that collision cross sections for different ion isotopes with the same velocity are identical until one reaches an energy low enough for quantum effects to become significant. To our knowledge, no theoretical calculations exist of this low energy for lithium-hydrogen ion collisions, but an estimate of not higher than 10 eV/u has been made [38]. Theoretical models of the isotope effect for hydrogen ion charge transfer collisions with beryllium atoms have been made and show an isotope effect at energies below 2 eV/u [39]. Our results indicate that the isotope effect in lithium-hydrogen collisions is negligible above 100 eV/u and in future experiments we aim to test for this effect at lower energies.

### C. Helium-lithium collision cross sections

One additional series of collision cross section measurements was undertaken with a study of collisions between singly charged helium ions and lithium atoms. The purpose of these measurements was to provide further comparison of our work with that of Varghese, to test for evidence of ionization collisions, and to search for undulations in the cross section for  $\text{He}^+$  impact on lithium. Figure 6 shows the results.

Our lithium-electron-loss cross sections are in excellent agreement with the charge transfer measurements of Varghese and with the theoretical predictions. The data shown in Fig. 6 are therefore consistent with a negligible ionization contribution in  $\text{He}^+ + \text{Li}$  collisions at energies below 3 keV. This is in agreement with a well-known feature of ion-atom collisions: that ionization cross sections become much smaller than charge transfer cross sections as the collision energy is reduced below some low value [42]. This has been quantified

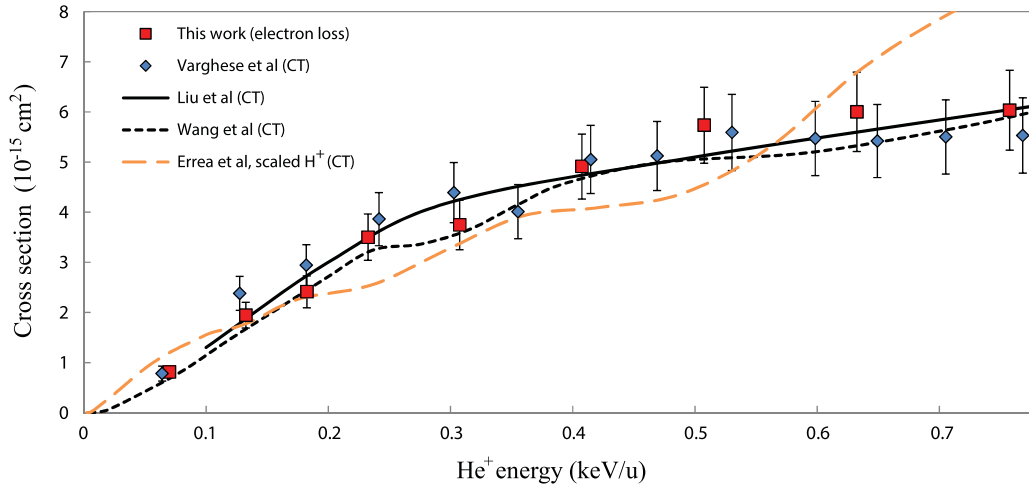


FIG. 6.  $\text{He}^+ + \text{Li}$  collision cross sections. Our work measures the lithium-electron-loss cross section while the work of Varghese *et al.* [16] measures the charge transfer cross section. Theoretical predictions for the charge transfer cross section are by Liu *et al.* [40] and Wang *et al.* [41]. Also shown are the theoretical cross section results for  $\text{H}^+ + \text{Li}$  from Errea *et al.* [20], scaled by a factor of 5.

for proton collisions with lithium [31] and sodium [43] atoms, where the ionization cross section is less than 10% of the capture cross section at energies below about 6 keV. There have been no previous measurements or theoretical predictions for lithium ionization due to  $\text{He}^+$  impact at low energy, but the data in Fig. 6 confirm ionization to be negligible compared to electron capture below 3 keV.

Undulations in the collision cross section can be seen in the quantum mechanical molecular-orbital close-coupling predictions of Wang *et al.*, and are identified as due to weak Stueckelberg oscillations [41]. These undulations appear to be matched by our experimental data in the energy range between about 0.2 and 0.4 keV/u. The atomic orbital close-coupling results of Lui *et al.* do not show such undulations, but this could in part be due to the coarse energy sampling in this work (only five cross sections are calculated in the energy range shown in Fig. 6). Also shown in Fig. 6 are the quantum mechanical molecular-orbital close-coupling cross sections of Errea *et al.* for proton charge transfer from lithium. These cross sections have been multiplied by a factor of 5 to allow comparison with the  $\text{He}^+ + \text{Li}$  cross sections. (The larger cross section for low energy  $\text{He}^+ + \text{Li}$  charge transfer compared to  $\text{H}^+ + \text{Li}$  is understood as due to a smaller energy defect for charge transfer in the  $\text{He}^+ + \text{Li}$  system [44].) By comparing the theoretical curves of Wang *et al.* and Errea *et al.* one can see that the undulations in the cross sections for proton and  $\text{He}^+$  impact do not track each other and, if anything, appear to be approximately out of step with one another. To discover if this is a coincidental relationship or the signature of an underlying connection between the collision dynamics of the  $\text{H}^+ + \text{Li}$  and  $\text{He}^+ + \text{Li}$  systems would require further theoretical analysis.

#### IV. CONCLUSIONS

We have detailed an experimental apparatus used to measure the lithium-electron-loss and charge transfer cross sections for collisions between ions and lithium atoms. The experimental technique used crossed beams of lithium atoms

and ions, unlike most prior experiments that passed the ion beam through a neutral atom gas cell. The crossed beams technique allowed efficient detection of the lithium ion produced in the collisions and could probe for impurities present in the lithium beam. In addition, the crossed beams technique enabled accurate measurements of the lithium target density by laser absorption spectroscopy.

Using this apparatus, we have measured cross sections for proton impact on lithium in the range 0.13–3 keV. Our results show good agreement with theoretical predictions throughout this energy range but below 0.7 keV our measured cross sections are significantly larger than the only previous experimental results. Our measured variation of cross section with collision energy shows a pronounced increase at about 0.85 keV due to charge transfer into the  $2p$  hydrogen orbital, while a more subtle increase at 0.18 keV was observed. The collision dynamics giving rise to this lower energy increase are unknown. Lithium-deuterium ion collisions were studied in the energy range 0.065–0.415 keV/u and gave collision cross sections consistent with those of lithium-proton collisions, as expected. Finally, we have measured lithium-electron-loss cross sections for singly charged helium impact on lithium between 0.07 and 0.75 keV/u. Our data are in excellent agreement with prior measurements and theoretical predictions for charge transfer collision cross sections, indicating that lithium ionization is a negligible process in this energy range. Undulations in the experimentally determined collision cross sections are seen to match those found in molecular-orbital calculations in the energy range 0.2–0.4 keV/u.

#### ACKNOWLEDGMENTS

We would like to thank several students from The College of the Holy Cross who participated in the early stages of the work presented here: P. Collins, K. Conte, J. Daly, M. Davis, S. Flaherty, B. Ptucha, and J. Wihbey. We would also like to thank J. Oxley for technical advice, D. Miller for machining expertise, and the College of the Holy Cross for student summer support.

- [1] G. B. Field and G. Steigman, Charge transfer and ionization equilibrium in the interstellar medium, *Astrophys. J.* **166**, 59 (1971).
- [2] T. E. Cravens, Comet hyakutake x-ray source: Charge transfer of solar wind heavy ions, *Geophys. Res. Lett.* **24**, 105 (1997).
- [3] R. C. Isler, An overview of charge-exchange spectroscopy as a plasma diagnostic, *Plasma Phys. Control. Fusion* **36**, 171 (1994).
- [4] C. H. Storry, A. Speck, D. Le Sage, N. Guise, G. Gabrielse, D. Grzonka, W. Oelert, G. Schepers, T. Seifick, H. Pittner, M. Herrmann, J. Walz, T. W. Hänsch, D. Comeau, and E. A. Hessels, First Laser-Controlled Antihydrogen Production, *Phys. Rev. Lett.* **93**, 263401 (2004).
- [5] R. P. Schorn, E. Hintz, D. Rusbuldt, F. Aumayr, M. Schneider, E. Unterreiter, and H. Winter, Absolute concentrations of light impurity ions in tokamak discharges measured with lithium-beam-activated charge-exchange spectroscopy, *Appl. Phys. B* **52**, 71 (1991).
- [6] M. Reich, E. Wolfrum, J. Schweinzer, H. Ehmler, L. D. Horton, J. Neuhauser, and A. U. Team, Lithium beam charge exchange diagnostic for edge ion temperature measurements at the ASDEX upgrade tokamak, *Plasma Phys. Control. Fusion* **46**, 797 (2004).
- [7] E. Wolfrum, F. Aumayr, D. Wutte, H. Winter, E. Hintz, D. Rusbuldt, and R. P. Schorn, Fast lithium-beam spectroscopy of tokamak edge plasmas, *Rev. Sci. Instrum.* **64**, 2285 (1993).
- [8] M. Sasao, K. A. Connor, K. Ida, H. Iguchi, A. A. Ivanov, M. Nishiura, D. M. Thomas, M. Wada, and M. Yoshinuma, Ion Sources for Fusion Plasma Diagnostics, *IEEE Trans. Plasma Sci.* **33**, 1872 (2005).
- [9] G. Z. Zuo, J. S. Hu, J. G. Li, N. C. Luo, L. E. Zakharov, L. Zhang, and A. Ti, First results of lithium experiments on EAST and HT-7, *J. Nucl. Mater.* **415**, S1062 (2011).
- [10] G. Z. Zuo, J. S. Hu, R. Maingi, Z. Sun, Q. X. Yang, M. Huang, X. C. Meng, W. Xu, Y. Z. Qian, C. L. Li, H. L. Bi, Y. Chen, X. L. Yuan, X. F. Han, X. Zhu, Y. F. Wang, L. Zhang, H. Q. Liu, L. Wang, X. Z. Gong *et al.*, and EAST team, Results from an improved flowing liquid lithium limiter with increased flow uniformity in high power plasmas in EAST, *Nucl. Fusion* **59**, 016009 (2019).
- [11] J. Ren, G. Z. Zuo, J. S. Hu, Z. Sun, Q. X. Yang, J. G. Li, L. E. Zakharov, H. Xie, and Z. X. Chen, A flowing liquid lithium limiter for the experimental advanced superconducting tokamak, *Rev. Sci. Instrum.* **86**, 023504 (2015).
- [12] F. L. Tabarés, Present status of liquid metal research for a fusion reactor, *Plasma Phys. Control. Fusion* **58**, 014014 (2016).
- [13] D. Andruczyk, R. Maingi, C. Kessel, D. Curreli, E. Kolemen, J. Canik, B. Pint, D. Youchison, and S. Smolentsev, A domestic program for liquid metal PFC research in fusion, *J. Fusion Energy* **39**, 441 (2020).
- [14] M. L. Apicella, G. Mazzitelli, V. Pericoli Ridolfini, V. Lazarev, A. Alekseyev, A. Vertkov, and R. Zagórski, First experiments with lithium limiter on FTU, *J. Nucl. Mater.* **363–365**, 1346 (2007).
- [15] D. P. Boyle, R. Majeski, J. C. Schmitt, C. Hansen, R. Kaita, S. Kubota, M. Lucia, and T. D. Rognlien, Observation of Flat Electron Temperature Profiles in the Lithium Tokamak Experiment, *Phys. Rev. Lett.* **119**, 015001 (2017).
- [16] S. L. Varghese, W. Waggoner, and C. L. Cocke, Electron capture from lithium by protons and helium ions, *Phys. Rev. A* **29**, 2453 (1984).
- [17] F. Aumayr and H. Winter, Total Single-Electron-Capture Cross Sections for Impact of  $H^+$ ,  $H^{2+}$ ,  $He^+$ , and  $Ne^+$  (2–20 KeV) on Li, *Phys. Rev. A* **31**, 67 (1985).
- [18] R. D. DuBois and L. H. Toburen, Electron capture by protons and helium ions from lithium, sodium, and magnesium, *Phys. Rev. A* **31**, 3603 (1985).
- [19] W. Grüebler, Charge Exchange Collisions between Hydrogen Ions and Alkali Vapour in the Energy Range of 1 to 20 KeV, *Z. Helvetica Physica Acta* **43**, 254 (1970).
- [20] L. F. Errea, F. Guzmán, L. Méndez, B. Pons, and A. Riera, Ab Initio Calculation of Charge-Transfer and Excitation Cross Sections in  $Li^+ + H(1s)$  Collisions, *Phys. Rev. A* **77**, 012706 (2008).
- [21] I. B. Abdurakhmanov, C. Plowman, A. S. Kadyrov, I. Bray, and A. M. Mukhamedzhanov, One-Center Close-Coupling Approach to Two-Center Rearrangement Collisions, *J. Phys. B: At. Mol. Opt. Phys.* **53**, 145201 (2020).
- [22] I. B. Abdurakhmanov, C. T. Plowman, K. H. Spicer, I. Bray, and A. S. Kadyrov, Effective single-electron treatment of ion collisions with multielectron targets without using the independent-event model, *Phys. Rev. A* **104**, 042820 (2021).
- [23] P. J. Salas, Electron Capture and Excitation Processes in the  $Li(2s; 2p\sigma, 2p\pi) + H +$  Collision (0.1–10 KeV), *J. Phys. B: At. Mol. Opt. Phys.* **33**, 3201 (2000).
- [24] R. Cabrera-Trujillo, J. R. Sabin, E. Deumens, and Y. Öhrn, Cross Sections for  $H^+$  and H Atoms Colliding with Li in the Low-KeV-Energy Region, *Phys. Rev. A* **78**, 012707 (2008).
- [25] W. Fritsch and C. D. Lin, Atomic Orbital Expansion Study of Electron Capture in  $H^+ + Li$  and  $He^{2+} + Li$  Collisions, *J. Phys. B: At. Mol. Phys.* **16**, 1595 (1983).
- [26] J. D. Thomas, G. S. Hodges, D. G. Seely, N. A. Moroz, and T. J. Kvale, Performance enhancement study of an electrostatic faraday cup detector, *Nucl. Instrum. Methods Phys. Res. A* **536**, 11 (2005).
- [27] J. M. Gerton, *Molecular Spectroscopy of a Bose-Einstein Condensate with Attractive Interactions*, Ph.D. thesis (Rice University, 2001).
- [28] G. Partridge (private communication).
- [29] P. Oxley and J. Wihbey, Precision atomic beam density characterization by diode laser absorption spectroscopy, *Rev. Sci. Instrum.* **87**, 093103 (2016).
- [30] M. Krems, J. Zirbel, M. Thomason, and R. D. DuBois, Channel electron multiplier and channelplate efficiencies for detecting positive ions, *Rev. Sci. Instrum.* **76**, 093305 (2005).
- [31] D. Wutte, R. K. Janev, F. Aumayr, M. Schneider, J. Schweinzer, J. J. Smith, and H. P. Winter, Cross Sections for Collision Processes of Li Atoms Interacting with Electrons, Protons, Multiply Charged Ions, and Hydrogen Molecules., *At. Data Nucl. Data Tables* **65**, 155 (1997).
- [32] D. H. Crandall, J. A. Ray, and C. Cisneros, Channeltron Efficiency for Counting of  $H^+$  and  $H^-$  at Low Energy, *Rev. Sci. Instrum.* **46**, 562 (1975).
- [33] J. Fricke, A. Müller, and E. Salzborn, Single particle counting of heavy ions with a channeltron detector, *Nucl. Instrum. Methods* **175**, 379 (1980).

- [34] G. E. Iglesias and J. O. McGarity, Channel Electron Multiplier Efficiency for Protons of 0.2–10 KeV, *Rev. Sci. Instrum.* **42**, 1728 (1971).
- [35] S. Takagi, Y. Kawasumi, N. Noda, and J. Fujita, Characteristics of a channel electron multiplier for detection of positive ion, *Jpn. J. Appl. Phys.* **22**, 1453 (1983).
- [36] D. W. Savin, L. D. Gardner, D. B. Reisenfeld, A. R. Young, and J. L. Kohl, In situ absolute calibration of a channel electron multiplier for detection of positive ions, *Rev. Sci. Instrum.* **66**, 67 (1995).
- [37] S. Shchemelinin, S. Pszona, G. Garty, A. Breskin, and R. Chechik, The absolute detection efficiency of vacuum electron multipliers, to KeV protons and  $\text{Ar}^+$  ions, *Nuclear Instruments and Methods in Physics Research A* **438**, 447 (1999).
- [38] L. Méndez (private communication).
- [39] P. Barragán, L. F. Errea, L. Méndez, I. Rabadán, and A. Riera, State selective electron capture and excitation in proton collisions with be, *J. Phys. B: At. Mol. Opt. Phys.* **41**, 225202 (2008).
- [40] L. Liu, J. G. Wang, and R. K. Janev, Spin-Resolved Electron Capture and Excitation Processes in  $\text{He}^+ - \text{Li}$  Collisions, *J. Phys. B: At. Mol. Opt. Phys.* **49**, 105201 (2016).
- [41] X.-X. Wang, K. Wang, Y.-G. Peng, C.-H. Liu, L. Liu, Y. Wu, H.-P. Liebermann, R. J. Buenker, and Y.-Z. Qu, Charge Transfer and Excitation Processes in Low Energy Collisions of  $\text{He}^+$  Ions with Li Atoms, *Res. Astron. Astrophys.* **21**, 210 (2021).
- [42] B. H. Bransden and M. R. C McDowell, *Charge Exchange and the Theory of Ion-Atom Collisions* (Oxford University Press, Oxford, 1992).
- [43] M. Zapukhlyak, T. Kirchner, H. J. Lüdde, S. Knoop, R. Morgenstern, and R. Hoekstra, Inner- and outer-shell electron dynamics in proton collisions with sodium atoms, *J. Phys. B: At. Mol. Opt. Phys.* **38**, 2353 (2005).
- [44] F. Aumayr, G. Lakits, and H. Winter, Electron capture and target excitation in slow ion-alkali atom collisions, *Z. Phys. D* **6**, 145 (1987).